Effect of few-walled carbon nanotube crystallinity on electron field emission property

Hae Deuk Jeong[1,2], Jong Hyeok Lee[1], Byung Gap Lee[1], Hee Jin Jeong[2], Geon-Woong Lee[2], Dae Suk Bang[1,♠], Donghwan Cho[1], Young-Bin Park[3] and Kwang Hwan Jhee[4]

[1]Department of Polymer Science and Engineering, Kumoh National Institute of Technology, Gumi 730-701, Korea
[2]Nano Carbon Materials Research Group, Korea Electrotechnology Research Institute, Changwon 641-120, Korea
[3]School of Mechanical and Advanced Materials Engineering, Ulsan National Institute of Science and Technology, Ulsan 689-798, Korea
[4]Department of Applied Chemistry, Kumoh National Institute of Technology, Gumi 730-701, Korea
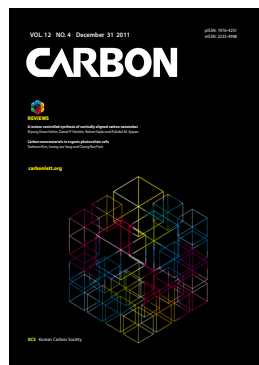
Abstract

We discuss the influence of few-walled carbon nanotubes (FWCNTs) treated with nitric acid and/or sulfuric acid on field emission characteristics. FWCNTs/tetraethyl orthosilicate (TEOS) thin film field emitters were fabricated by a spray method using FWCNTs/TEOS sol one-component solution onto indium tin oxide (ITO) glass. After thermal curing, they were found tightly adhered to the ITO glass, and after an activation process by a taping method, numerous FWCNTs were aligned preferentially in the vertical direction. Pristine FWCNT/TEOS-based field emitters revealed higher current density, lower turn-on field, and a higher field enhancement factor than the oxidized FWCNTs-based field emitters. However, the unstable dispersion of pristine FWCNT in TEOS/N,N-dimethylformamide solution was not applicable to the field emitter fabrication using a spray method. Although the field emitter of nitric acid-treated FWCNT showed slightly lower field emission characteristics, this could be improved by the introduction of metal nanoparticles or resistive layer coating. Thus, we can conclude that our spray method using nitric acid-treated FWCNT could be useful for fabricating a field emitter and offers several advantages compared to previously reported techniques such as chemical vapor deposition and screen printing.

Key words: carbon nanotube, tetraethyl orthosilicate, field emitter, spray coating

1. Introduction

Carbon nanotubes (CNTs) have many exceptional properties that make them attractive for a variety of applications. Previous works have shown that CNTs have novel physical and chemical properties making them promising materials in field emission devices. In 1995, four years after the discovery of CNTs by Iijima [1], three groups reported field emission from CNTs at low turn-on fields and high current densities [2]. From 1998, the concept of using nanotubes in field emission devices spurred on efforts worldwide: a first display [3] as well as a lighting element [4] was presented. This area has been experiencing a rapid growth the past few years, and it is encouraging to note that two commercial products, namely high-brightness luminescent elements and an X-ray tube, have hit the market. Applications such as flat displays [4], X-ray tube sources [5,6], electron sources for high-resolution electron beam instruments such as electron beam lithography machines and electron microscopes [7,8] are under active consideration.

There are several properties of CNTs that make them extraordinary materials for field emission. Firstly, the graphene walls in them are parallel to the filament axis resulting in the nanotubes (whether metallic single-walled or multi-walled) exhibiting high electrical conductivity at room temperature. Secondly, CNTs are high in aspect ratio and whisker-like

in shape. Utsumi [9] evaluated commonly used field emission tip shapes and concluded that the best field emission tip should be whisker-like, followed by the sharpened pyramid, hemispheroidal, and pyramidal shapes. It has been reported that even curly 'spaghetti-like' nanotubes stand up vertically like whiskers during emission under the application of an electric field [10]. Thirdly, CNTs can be very stable emitters, even at high temperatures. Previous researchers demonstrated that a multi-walled carbon nanotube (MWCNT) emitter could be heated up to 2000 K by its field-emitted current and remain stable. They claimed that this was the first reported observation of field emission induced stable heating. This characteristic is distinctively different from metal emitters. In metals, the resistance, R, increases with temperature, which means that more heat, Q, is produced as higher currents, I, are drawn ($Q = I^2R$). The combination of high temperature and electric field causes the well-known mechanism of field-sharpening of tips by surface diffusion, which in turn increases the local field, current. and temperature. This positive feedback mechanism causes an unstable thermal runaway, which inevitably leads to emitter destruction for metal-based emitters. In contrast, the resistance of a CNT decreases with temperature, which limits I^2R heat generation. Consequently, its temperature varies sub-linearly with the current [11]. Additionally, surface diffusion is less likely in the strong C-C covalent bonds of the CNTs. These unique characteristics of CNTs make them a remarkable field emitter.

In general, single-walled carbon nanotubes (SWCNTs) have been studied to obtain low threshold electric field and high emission current density [12], but abrupt degradation of emission current becomes a serious obstacle for field emission applications. In contrast to SWCNTs, MWCNTs have shown better emission stability; however, a small field enhancement factor has been attributed to low emission current [13]. Recently, double-walled carbon nanotubes have been studied for this purpose due to high current density with long-term emission stability, but the poor production rate and following purification process of catalysts have been a serious bottleneck [14]. Few-walled carbon nanotubes (FWCNTs), with small number of walls (2 to 6) and small diameters (below 5 nm), have been synthesized with high catalyst efficiency such that no further purification process was required [15]. Therefore, these FWCNTs could be the most promising candidates for the field emitter due to their intermediate structural properties between SWCNTs and MWCNTs [16] and high production rate.

To fabricate CNT field emitters, there are several available methods including direct growth of CNT arrays using chemical vapor deposition (CVD), paste screen-printing of CNT powders, and electrophoretic deposition. However, each of them has several problems. The catalyst CVD method has to be performed at a higher temperature for CNT growth. Its fabricating process is limited by the scalability of the substrate size and it is difficult to control CNT morphologies such as density and spacing. The paste screen-printing method, by contrast, is known as a more effective technology for large-scale production and has the advantage of a low cost process. However, substantial degradation of emission tips caused by oxygen gases that are out-gassed from the organic vehicles in the paste cannot be avoided and as a result, poor uniformity of emission, poor emission spot density, and short lifetime will limit its application in commercial pro-

duction. Furthermore, because the vapor from residual organic solvent will severely deteriorate the vacuum of field emission devices after the sealing process, a post-heat-treatment to remove the residual organic solvent from the paste is necessary. The electrophoretic method has the problems of weak adhesion between CNT emitters and substrates, and non-uniformity in the thickness of the deposited layer, which will cause irregularity in the distribution of emission sites. The spray method is an easy and convenient method to deposit CNTs on the cathode substrates with a large area. However, the poor adhesion of CNTs to the substrate is also a serious drawback for long-term electron emission. Moreover, the spray method has been largely hampered by poor dispersion of CNTs, which was caused by their inherent attractive van der Waals interactions between CNTs. One of the best methods to overcome this problem is to introduce carboxyl groups (-COOH) and hydroxyl groups (-OH) onto the surface of the CNTs through oxidation by nitric acid/sulfuric acid treatment. While this technique is a powerful method for improving the dispersion of CNTs, the acid treatment induces structural defects that change the property and morphology of CNTs.

In this study, we describe the fabrication of the CNT cathodes by a spray method using a FWCNTs/binder one-component solution to improve the adhesion between the FWCNTs and the substrate for long-term emission stability. Moreover, various oxidation processes were applied to modify the surfaces of pristine FWCNTs. The hydration properties of FWCNTs and their effects on electron field emission property were studied.

2. Experimental

2.1. Materials

The FWCNTs fabricated by CVD method were purchased from Hanwha Nanotech Co. We used a CNT product (CMP series) consisting of highly purified agglomerates of FWCNTs with an outer mean diameter of 3 to 5 nm and a typical length ranging from hundreds of nanometers to a micrometer. Tetraethyl orthosilicate (TEOS) was purchased from Aldrich and used as received for improving adhesion between the FWCNTs and the substrate. Sulfuric acid (H_2SO_4) and nitric acid (HNO_3) (Daejung Chemicals Co., Korea) were used for functionalization of CNTs on their side wall by chemical oxidation process. We used N,N-dimethylformamide (DMF) as a dispersion solvent of CNTs due to the high value of dispersion component (δ_d) of the Hildebrand solubility parameter (δ_t). Ham et al. [17] noted that solvents with high values of δ_d are the best for making homogeneous and agglomerate-free dispersions of CNTs.
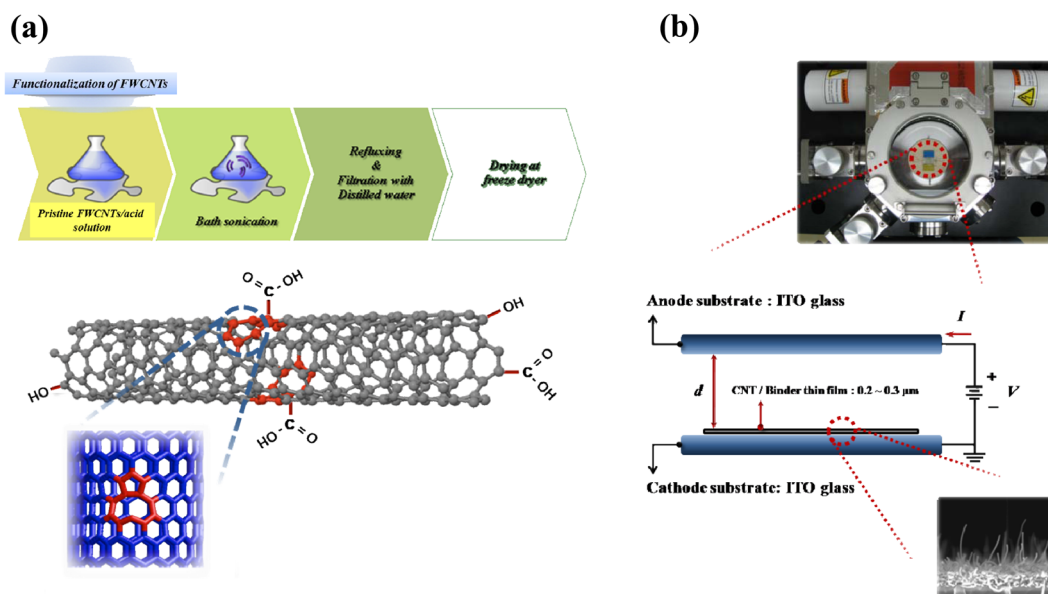
2.2. Surface functionalization of FWCNTs

For the surface functionalization of FWCNTs, 50 mg of the agglomerated FWCNTs were mixed with 100 mL of one of the acid solutions listed in Table 1 by stirring for 5 min at room temperature and sonicating in a conventional ultrasonic bath (100 W) for 10 min; sonication longer than 10 min with high

Table 1. Acid treatment conditions for each sample

Sample	Acid condition	FWCNTs conc. (g/L)	Sonic. time (min)	Refluxing time (min)	Refluxing temp. (°C)
Pristine FWCNT	-	-	-	-	-
N_FWCNT	HNO$_3$ 70%	0.5	10	60	150
SN-a FWCNT	H$_2$SO$_4$/HNO$_3$_3/1	0.5	10	15	150
SN-b FWCNT	H$_2$SO$_4$/HNO$_3$_3/1	0.5	10	30	150

FWCNT: few-walled carbon nanotube.

(a)

(b)

Fig. 1. (a) Schematic of the acid treatment process for functionalization on FWCNTs surface and (b) illustration of the vacuum tube diode field emission test setup. FWCNT: few-walled carbon nanotube, ITO: indium tin oxide.

power could induce surface defects, not a functionalization, of FWCNTs. The sonicated FWCNTs/acid mixture was refluxed on a hot plate at 150°C and then the slurry was filtered by vacuum filtration using an alumina filter and thoroughly washed with distilled water until the solution reached a pH value of 7. Finally, the functionalized FWCNTs were dried by a freeze dryer for 48 h to remove moisture. Fig. 1a describes the acid treatment process schematically.

2.3. Preparation of FWCNTs/TEOS sol one-component solution

TEOS sol solution was prepared by mixing 5 g of tetraethoxy silane, 1.73 g of water, 3.33 g of ethanol, and 8 mg of 30.9 M hydrochloric acid, and performing a continuous sol-gel reaction at 60°C under 250 rpm (Table 2). After that, pristine and functionalized FWCNTs were dispersed in the DMF for 2 h in a conventional ultrasonic bath (100 W) at a definite concentration. Next, we centrifuged the solution 5000 rpm for 30 min to remove graphitic particles and large CNT bundles. Lastly, dispersed FWCNTs solution was mixed with TEOS sol and sonicated in a conventional ultrasonic bath (100 W) for 30 min (Table 3).

Table 2. Formulation of the TEOS sol

TEOS : H$_2$O (mol : mol)	EtOH (wt%) (Basis; TEOS solid content)	HCl conc. (M)
1 : 4	65	30.9

TEOS: tetraethyl orthosilicate, HCl: hydrochloric acid.

Table 3. Formulation of the FWCNTs/TEOS one component solution for spray coating

FWCNTs conc. (mg/L)	FWCNTs/TEOS (w/w)	Solvent
100	1/1	DMF

FWCNT: few-walled carbon nanotube, TEOS: tetraethyl orthosilicate, DMF: *N,N*-dimethylformamide.

2.4. Preparation of FWCNTs/TEOS thin film field emitter

The field emitters using FWCNTs/TEOS one component solution were prepared by the following method. Firstly, the FWCNTs/TEOS one component solution was sprayed onto in-

dium tin oxide (ITO) coated glass by an automatic spray coater (NVD-200, Fujimori, Japan) with a nozzle of 1.2 mm diameter at 135°C. The prepared FWCNTs/TEOS thin films (2 × 2 cm²) were then cured in a vacuum oven at 150°C for 90 min. After thermal curing, they were found tightly adhered to the ITO glass. We performed the activation process by a taping method that creates many nanotubes aligned in the vertical direction.

2.5. Characterizations

To get information about functional groups on the nanotube surface, X-ray photoelectron spectroscopy (XPS) measurements were performed on a MultiLab2000 (Thermo VG Scientific, UK) with monochromatized Al Kα X-ray radiation as the X-ray source for excitation under ultrahigh vacuum system. The XPS core level spectra were analyzed with a fitting routine, which can decompose each spectrum into individual mixed Gaussian Lorentzian peaks. Raman spectroscopy (FRS-100S; Bruker, USA) with an Ar laser excitation of 633 nm wavelength was used to assess the quality of the graphitic structure of the FWCNTs. We measured the Raman spectrum from more than ten different points of each sample for correct information. The corresponding images of the samples were obtained by field-emission scanning electron microscopy (FE-SEM, 10 kV, S-4800, Hitachi, Japan). The well-dispersed FWCNTs solution after centrifugation was analyzed by UV visible (UV-VIS) spectroscopy (cary 5000; Varian, USA) to determine the effect of acid treatment on the state of the dispersion and dispersability of the nanotubes in DMF.

The field emission properties were measured in a diode type with a direct current bias inside a vacuum chamber under less than 5 × 10⁻⁷ Torr of pressure, as shown in Fig. 1b. ITO glass was used as an anode electrode separated by a 200 μm polyethylene terephthalate (PET) spacer. To obtain stable field emission properties, an electrical aging process was performed by the following method: first, 100 repetitions of I-V sweeping up to 0.5 mA/cm² of emission current density, then constant voltage annealing at 0.35 mA/cm² of emission current density for 2 h.

During this electrical aging process, some protruded FWCNTs were removed so that the length uniformity of FWCNT emitters was enhanced, which resulted in stable electron emission. White phosphor-coated ITO glass as an anode was used to determine the emission pattern of FWCNT emitters.

3. Results and Discussion

3.1. Characterization of pristine and acid-treated FWCNTs

3.1.1. XPS analysis of FWCNTs

With reference to functionality grafting, XPS is a surface analytical technique that can provide useful information on the nature of functional groups and also on the presence of structural defects on the nanotube surface. The intensity I of photoelectrons of kinetic energies E is given by [18]:
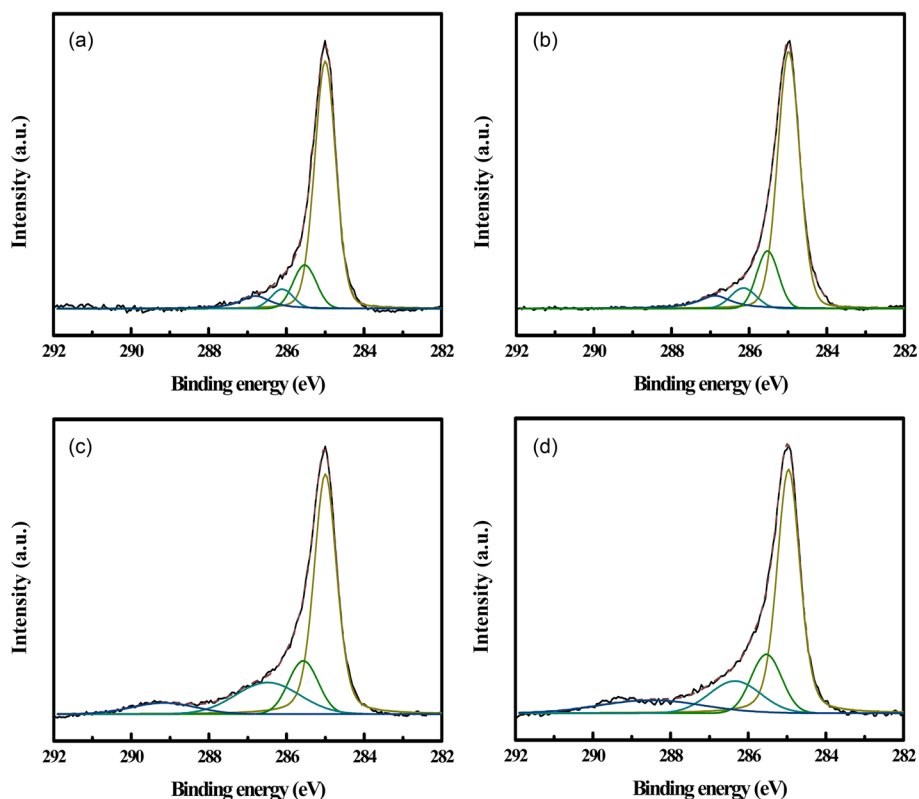
Fig. 2. Deconvolution of the X-ray photoelectron spectroscopy C₁ₛ peak for the (a) pristine FWCNT, (b) N_FWCNT, (c) SN-a FWCNT and (d) SN-b FWCNT. FWCNT: few-walled carbon nanotube.

Table 4. Relative percentage of functional components obtained from curve fitting the C1s peak for the pristine FWCNT and oxidized FWCNTs

Sample	Surface functional groups and their relative percentages (%)			
	C-C	C-O	C=O	O-C=O
Pristine FWCNT	74.48	12.96	5.62	6.94
N_FWCNT	72.22	14.40	6.10	7.28
SN-a FWCNT	59.26	14.87	19.07	6.80
SN-b FWCNT	57.47	15.96	14.66	11.91

FWCNT: few-walled carbon nanotube.

Table 5. Summary of the elemental composition for the pristine FWCNT and oxidized FWCNTs

Sample	Element (at. %)	
	C	O
Pristine FWCNT	99.23	6.77
N_FWCNT	92.75	7.25
SN-a FWCNT	86.10	13.90
SN-b FWCNT	85.86	14.14

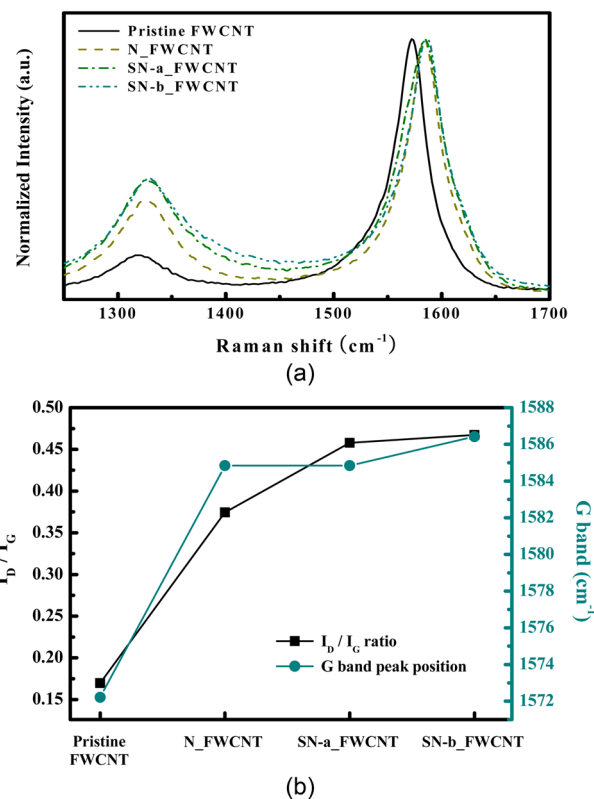FWCNT: few-walled carbon nanotube

$$I = N\sigma\lambda(E)T(E), \tag{1}$$

where N is the atomic density, σ is the ionization cross-section of the observed photoelectron line according to a defined core level and the photon energy $h\nu$, $\lambda(E)$ is the inelastic mean free path, and $T(E)$ is the transmission function of the spectrometer used. Thus, $I \propto N$, and we can quantitatively analyze the atomic concentration of carbon atoms functionalized in the oxidizing process. Atomic composition of functionalities was obtained from curve fitting results based on ratios of peak areas. These values could only give us basic information about the functional groups attached to nanotubes.

The C1s peak of pristine and acid-treated FWCNTs at 285 eV can be deconvoluted into four fitting curves with binding energy at ~285 eV, ~285.63 eV, ~286.59 eV, and ~289.16 eV, which are assigned to C-C, C-O, C=O and O-C=O, respectively (Fig. 2) [19]. The relative amount of functional groups could be calculated from the area of each deconvoluted peak. The relative amount of functional groups and the atomic element in the samples is listed in Tables 4 and 5, respectively.

As seen in Table 4, we found that the relative amounts of C-O and O-C=O on the surface of acid-treated FWCNTs are higher than that of pristine FWCNT. Furthermore, sulfuric/nitric acid-treated FWCNTs (indicated by SN-a FWCNT and SN-b FWCNT) have much higher relative amounts of C-O and O-C=O than nitric acid-treated FWCNT (indicated by N_FWCNT). Moreover, the atomic percentage of the oxygen element (Table 5) on the surface of acid-treated FWCNTs noticeably increases compared to pristine FWCNT. These results indicate that acid treatment with sulfuric/nitric mixture acid could effectively in-

(a)

(b)

Fig. 3. (a) Raman spectra (excitation at λ = 633 nm) for pristine few-walled carbon nanotube (FWCNT) and oxidized FWCNTs at various acid treatment conditions. (b) Ratio of the D-to-G band intensity and the G band shift.

duce more polar oxygen-containing groups on the surface of nanotubes, which will improve the stability of CNT dispersion in DMF.

3.1.2. Carbon ordering

Raman spectroscopy is a powerful measurement method for evaluating the structural properties of CNT because it is a non-destructive and contactless measurement method. The CNT was formed through the crimping of flat graphite and has an unsaturated double-bond structure on the graphitic structure; thus a characteristic band can be measured using the Raman spectra. The peak near 1580 cm^{-1} represents the graphite E_{2g} symmetry of the interlayer mode, which reflects the structural intensity of the sp^2 hybridized carbon atoms of the CNTs, and the absorption peak is referred to as the G band (graphitic band). A perfect graphitic sheet is composed of hexagons of carbon atoms, and when pentagons and heptagons or defects occur in other positions, defect D bands (disorder band) can take place at 1350 cm^{-1}; the D band accounts for the crystal defect degree of graphitic sheets. Therefore, the extent of the defects in CNTs can be evaluated by the ratio of the D and G band intensities (I_D/I_G).

In this study, Raman spectroscopy was used to assess the quality of FWCNTs depending on the acid treatments. Fig. 3a shows the Raman spectrum of pristine and acid-treated FWCNTs. The maximum Raman peak near 1570 cm^{-1} (G band) related to the graphite E_{2g} symmetric intra-layer mode was shifted to higher wavenumbers after acid treatment (Fig. 3b). This phenomenon

could be explained by the following two reasons. First, when the CNTs are treated by nitric acid or sulfuric/nitric acid π electrons are withdrawn from the nanotube to nitrate ions (NO_3^-), which resulted in the blue shift of Raman G band [20]. Second, it has been reported that the tangential Raman E_{2g} mode can be shifted to higher wavenumbers upon hydrostatic pressure, which corresponds to a reduction in the bond length and an associated stiffening of the bonds [21]. In our experiment, compressive strain of the C-C bond or a change in the bond angles resulting from graphitic layer stacking caused by strong hydrogen bonding could lead to an up-shift in the tangential mode frequency. In this case, we believe the strong intermolecular interaction between hydroxyl groups could have arisen from the acid treatment, thus enhancing graphitic layer stacking.

In addition, as shown in Fig. 3b, sulfuric/nitric acid-treated samples (SN-a FWCNT, SN-b FWCNT) have a higher I_D/I_G ratio than the nitric acid-treated sample (N_FWCNT), and the I_D/I_G ratio increases with increased refluxing time. These results indicate that the crystallinity of nanotubes could be triggered by a strong acid treatment and its experimental condition. In general, defects in nanotubes are mainly located at the tip due to the hemisphere structure of the carbon buckyball. Some defects can form on the side wall of the nanotube because of bending or kinking. These defects can be oxidized by a strong acid and then chemical functionalization can easily occur. Furthermore, these side wall defects can be an electron trapping site, which can be attributed to poor electron emission, even though the open tip of a nanotube has better emission properties than a closed one. In the Section 3.2, we will discuss the effects of nanotube crystallinity on field emission properties.

3.1.3. Solubility and stability of FWCNT dispersion in DMF

It is well known that the bundled structure of nanotubes does not actively absorb light in the UV-Vis region; individual nanotubes show the opposite effect [22]. Therefore, dispersion of CNTs can be characterized using UV-Vis absorption spectroscopy. In this study, to characterize the dispersion of FWCNTs in DMF using UV-Vis spectroscopy, absorbance values were recorded at 550nm, as reported in previous studies [23,24], which is shown in Fig. 4. According to the Beer-Lambert's law ($A = \log I_0/I = \varepsilon Cl$), the absorbance A is expressed in terms of extinction coefficient ε, the concentration of nanotubes C, and the light path length l. In general, the absorbance is measured from absorption spectroscopy at a given wavelength. The path length l is fixed for a given optical cell in the experiment. Therefore, if the concentration of the CNT in solution is known, the extinction coefficient can be easily obtained using the equation.

Fig. 4a depicts the UV-Vis spectra of pristine and oxidized FWCNTs solution with various concentrations of nanotubes in DMF. We note that the relationship between the absorbance and the concentration of the FWCNT solutions was linear, which is in good agreement with Beer-Lambert's law [25]. In addition, it is noteworthy that the UV absorbance value of pristine FWCNT solution was higher than that of the oxidized FWCNTs solution; therefore, the extinction coefficient of the pristine FWCNT solution at a nanotube concentration of 100 mg/L is the largest (Fig. 4b). We note that the absorbance of the nitric acid-treated sample (N_FWCNT) was higher than that of the sulfuric/nitric acid-treated samples (SN-a FWCNT, SN-b FWCNT) at the
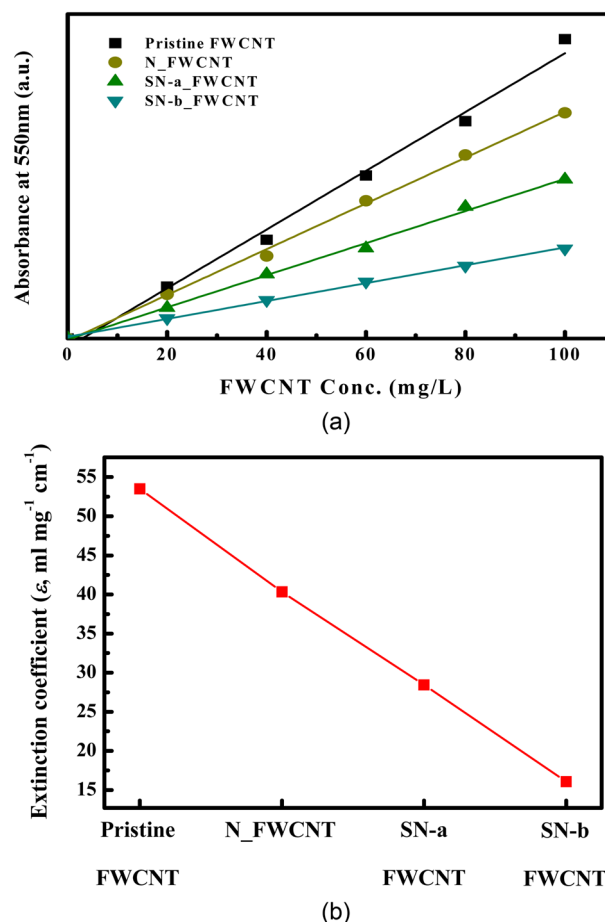
Fig. 4. (a) UV-visible absorbance at 550 nm for pristine and oxidized few-walled carbon nanotubes (FWCNTs) solutions depending on the acid treatment at the same FWCNTs concentration and (b) extinction coefficient at 550 nm for pristine and oxidized FWCNTs solutions depending on the acid treatment at the same FWCNTs concentration (100 mg/L).

same nanotube concentration (Fig. 4). In general, carbon atoms in the pristine CNTs are in an sp^2 state, but an sp^3 carbon configuration is generated during the oxidization in the defect sites of CNTs. The geometrical tension between the hybridization of oxidized and non-oxidized carbon induced local deformations. One would expect that extended acid treatment, in which a greater number of functional groups are produced, would be accompanied by more deformation. Therefore, we believe that this phenomenon is due to the bent, shortened, and bundled structure in several areas resulting from the acid treatment.

Fig. 5 shows the visual examination of pristine and oxidized FWCNTs in DMF at a nanotube concentration of 100 mg/L and 200 mg/L, respectively. Digital photo-images were taken after 24 h. It was found that the clear dispersion of pristine FWCNT in DMF was formed when the nanotube concentration was 100 mg/L, but in a higher concentration of 200 mg/L, the nanotubes were aggregated and precipitated. On the other hand, the oxidized FWCNTs showed a clear dispersion independent of the nanotube concentration in DMF. The stability of oxidized FWCNTs in DMF may be due to the fact that the oxidation process introduces carboxyl and hydroxyl groups on the nanotube sur-
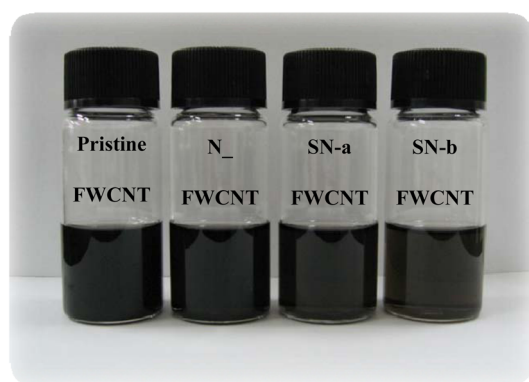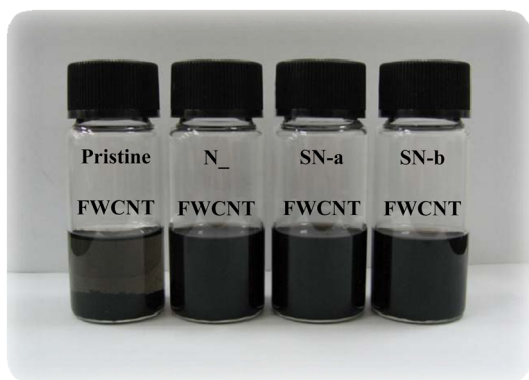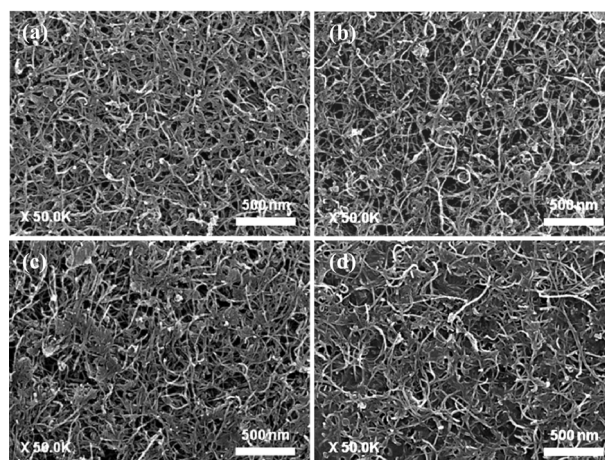
Fig. 5. Digital photo-images of pristine and oxidized few-walled carbon nanotubes (FWCNTs) dispersed in N-dimethylformamide at nanotube concentrations of (a) 100 mg/L and (b) 200 mg/L, respectively. Pictures were taken after 24 h.

Fig. 6. Field-emission scanning electron microscopy images of (a) pristine FWCNT/TEOS, (b) N_FWCNT/TEOS, (c) SN-a FWCNT/TEOS and (d) SN-b FWCNT/TEOS based field emitters before the surface activation, respectively. FWCNT: few-walled carbon nanotube, TEOS: tetraethyl orthosilicate.

Fig. 7. Cross sectional field-emission scanning electron microscopy images of (a) pristine FWCNT/TEOS, (b) N_FWCNT/TEOS, (c) SN-a FWCNT/TEOS and (d) SN-b FWCNT/TEOS based field emitters before the surface activation, respectively. FWCNT: few-walled carbon nanotube, TEOS: tetraethyl orthosilicate.

faces. These groups ionize in DMF and the oxygen-containing groups are negatively charged. The electrostatic repulsive forces between negative surface charges of the oxygen-containing groups may lead to the stability of oxidized nanotubes so that the oxidized nanotubes can form a stable dispersion in DMF. This suggests that the oxidized FWCNTs have high dispersion stability in DMF so that the aggregation could be minimized. Consequently, when the CNTs are oxidized by an acid treatment, the dispersion stability in DMF is significantly enhanced due to the combination of polar-polar affinity and electrostatic repulsion.
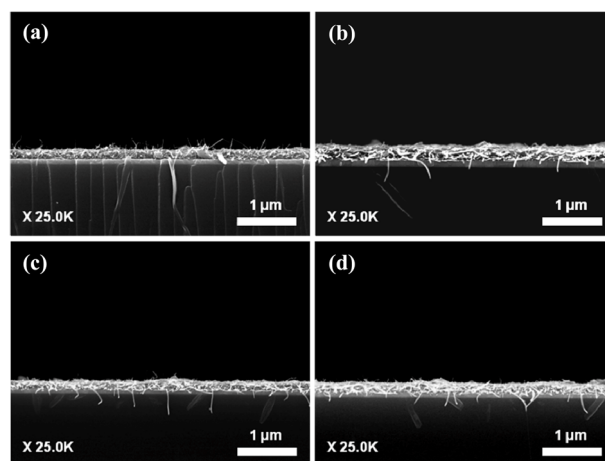
3.2. Characterization of FWCNTs/TEOS thin film field emitter

3.2.1. Morphological property

Fig. 6 shows the FE-SEM images of the spray coated FWCNTs/TEOS films before the activation process. As increasing the oxidation level (or I_D/I_G), the TEOS binder was shown in the top of the film. The intermolecular interaction of TEOS with nanotubes is quite poor, so that the TEOS binder should be precipitated to the bottom of the film. However, CNTs functionalized with carboxyl or hydroxyl groups could interact with the TEOS layer precipitated to the bottom of the film, which is very low in the case of highly oxidized sample, as shown in the Figs.

6c and d. We also realized that the adhesion strength between CNTs and the substrate is varied depending on these oxidation levels. Therefore, following the activation process using the taping should be optimized to minimize this adhesion effect on the field emission of CNTs.

Figs. 7 and 8 show the cross-sectional FE-SEM image of the spray coated FWCNTs/TEOS-based field emitter before and after the activation process. The thickness of FWCNTs/TEOS film was about 0.3 µm. It was difficult to observe the protruded CNTs at the film surface before the activation process. The buried nanotubes on the surface have been aligned by the removal of a covered layer, by applying the adhesive tape technique. As explained previously, this taping process was individually optimized to all samples. The surface morphology of activated FWCNTs/TEOS-based field emitter is shown in Fig. 8. After the
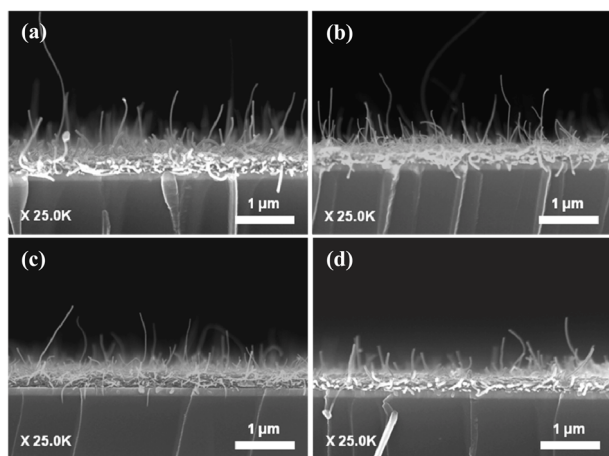
Fig. 8. Field-emission scanning electron microscopy images of (a) pristine FWCNT/TEOS, (b) N_FWCNT/TEOS, (c) SN-a FWCNT/TEOS and (d) SN-b FWCNT/TEOS based field emitters cross-section after the surface activation, respectively. FWCNT: few-walled carbon nanotube, TEOS: tetraethyl orthosilicate.

activation process, the film thickness slightly decreased from its original value of about 0.3 μm to about 0.2 μm, and many CNTs were preferentially aligned to the vertical direction. The aligned nanotube density of pristine FWCNT (Fig. 8a), nitric acid-treated FWCNT (Fig. 8b) and FWCNTs treated with sulfuric/nitric acid for a short time (Fig. 8c) is quite similar, but the FWCNTs treated by sulfuric/nitric acid for a long time (Fig. 8d) have low aligned nanotube density even though we sprayed the same amount of nanotube solution and optimized the activation process. The vertical alignment of the nanotube is necessary for its field emission application because high field enhancement is strongly related to the aspect ratio of the nanotube in the vertical direction. The emission stability of CNT emitters is also enhanced after the activation process because some loosely bounded nanotubes could be efficiently removed.

Therefore, the activation process of the CNT film is an important step in making a high performance nanotube field emitter. Vertically aligned CNT emitters are aged electrically inside a vacuum chamber to produce a uniform length distribution, which results in the stable emission of electrons even at a high electric field. During this electrical aging step, some protruded nanotube emitters, as shown in the Figs. 8a and b are oxidized through Joule heating.

3.2.2. Field emission properties of FWCNTs/TEOS thin film field emitter

Field emission results are usually analyzed by the *Fowler-Nordheim* (*F-N*) theory, which describes the emission of electrons from a metal as quantum-mechanical tunneling enhanced by a strong electric field [26-28]. The *F-N* equation can be written as:

$$J = \frac{AE^2}{\phi t^2(y)} \exp\left[-B\frac{\phi^{3/2}}{E}v(y)\right],$$ (2)

where J is the current density, E is the electric field strength, ϕ is the work function, and A and B are constants (when J, E and ϕ are expressed in mA/cm^2, V/cm and eV, respectively, the con-
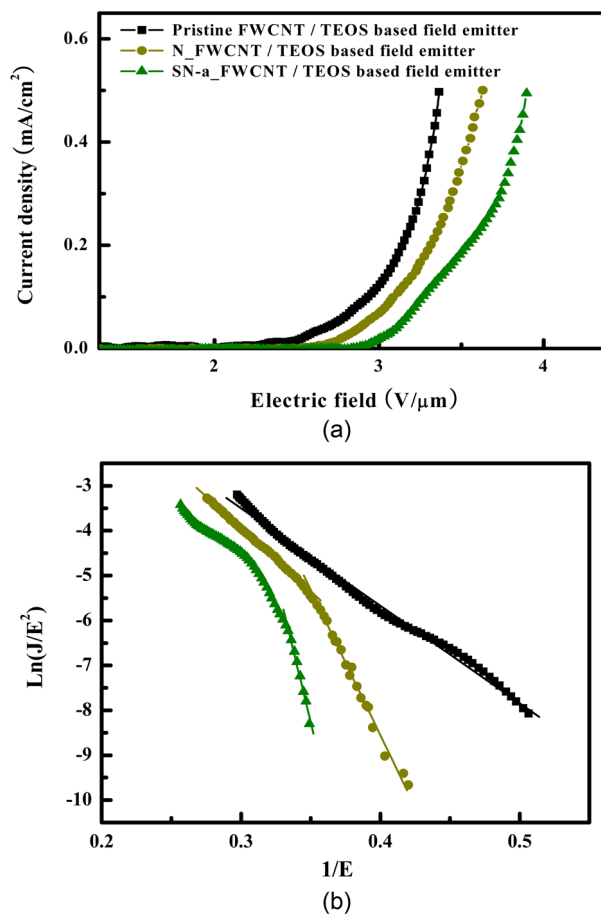
Fig. 9. (a) J-E characteristics and (b) their Fowler-Norheim plot of the pristine FWCNT/TEOS and oxidized FWCNTs/TEOS based field emitters. FWCNT: few-walled carbon nanotube, TEOS: tetraethyl orthosilicate.

stants A and B assume the values of 1.54×10^{-6} A·eV/V^2 and 6.87×10^7 V/cm·eV$^{3/2}$, respectively). According to the *F-N* model, a plot of ln (I/V^2) vs. I/V has a linear behavior with a slope that can used to evaluate the field enhancement factor (β).

The field emission characteristics of pristine and oxidized FWCNTs were measured after electrical aging in each sample as shown in Fig. 9 and Table 6. The vertically aligned pristine FWCNT/TEOS field emitter shows a low turn-on voltage of 1.90 V/μm, high field enhancement factor of 3519.43, and high emission current density of 0.5 mA/cm^2 at an applied field of about 3.37 V/μm. On the other hand, the nitric acid-treated FWCNT/TEOS (N_FWCNT) field emitter shows a turn-on voltage of 2.38 V/μm, field enhancement factor of 1055.24, and emission current density of 0.5 mA/cm^2 at an applied field of about 3.63 V/μm. A more excessively acid-treated FWCNT (SN-a FWCNT) compared to N_FWCNT shows the turn-on voltage of 2.83 V/μm, field enhancement factor of 580.23, and emission current density of 0.5 mA/cm^2 at an applied field of about 3.9 V/μm. The field emission of FWCNT treated with sulfuric/nitric acid for a long time (SN-b FWCNT) was not observed due to the low aligned nanotube density and high defect ratio. The oxidized FWCNTs-based field emitter indicates higher turn-on voltage than the pristine FWCNT-based field emitter because

Table 6. The ratio of the D-to-G band intensity and field emission characteristics of the pristine FWCNT/TEOS and oxidized FWCNTs/TEOS based field emitters

Sample	I_D / I_G ratio	E turn-on (V/μm)	E J = 0.5 $_{mA/cm^2}$ (V/μm)	β
Pristine FWCNT	0.17	1.90	3.37	3519.43
N_FWCNT	0.37	2.38	3.63	1055.24
SN-a FWCNT	0.45	2.83	3.90	580.23
SN-b FWCNT	0.47	-	-	-

Turn-on field was calculated as a starting field of the linear region at the Fowler-Norheim (F-N) plot. The field enhancement factor was determined from the slope of the linear region, β = -Bφ1.5 / S where B is just a constant, φ is the work function, and S is the slope of the F-N plot. We assumed the work function of the nanotube to be 5.0 *eV*. FWCNT: few-walled carbon nanotube, TEOS: tetraethyl orthosilicate.

of the defects on the nanotube surface. There are two possible explanations. First, the defects located on the side wall of nanotubes can act as an electron trapping site. It is well known that in an ideal nanotube, ballistic electron transfer is realized. That is why the electrical conductivity of nanotubes is extremely high. However, when the nanotube is treated with a strong acid, defects are formed in its side wall, and then the electrons are scattered and/or trapped. Finally, the conductivity of a defective nanotube is lower than that of an ideal one. In the field emission, the conductivity of emitters is also a very important physical property. Second, vertical alignment of nanotubes could be altered by a defect. The defects in the side wall of the nanotube mean that pentagons and heptagons are generated, and this results in the bending of the nanotube with a certain angle to the vertical nanotube axis. In general, it is well known that vertically aligned nanotubes have much lower turn-on voltage and higher field enhancement factors than randomly entangled CNTs, indicating that most electrons are emitted from the tips of FWCNTs and the electronic DOS of tips near the Fermi energy is different from that of side walls [29]. Therefore, vertically aligned CNTs without defects can be used as highly effective field emitters.

The *F-N* plot is shown in Fig. 9b. To calculate the field enhancement factor (*β*), we use the *F-N* equation. When assuming the work function of CNTs to be 5.0 eV, the pristine FWCNT-based field emitter showed the higher field enhancement factor (*β*) of 3519.43 compared to the oxidized FWCNTs. We can consider that the field enhancement factor is strongly related to the aspect ratio of nanotubes in the vertical direction. As mentioned above, a defective nanotube is bent and thus the vertical height is smaller compared to an ideal one. Also, the bundled structure is enhanced upon acid treatment due to the strong interaction of functional groups. Therefore, the aspect ratio of acid-treated FWCNTs is smaller than that of pristine FWCNT, which explains the high field enhancement factor for pristine FWCNT. It is worth noting that the field emission properties of acid-treated FWCNT at a high electric field are different from those at a low electric field. The field emission properties of acid-treated FWCNT are significantly enhanced at high electric field. There are

(a)

(b)
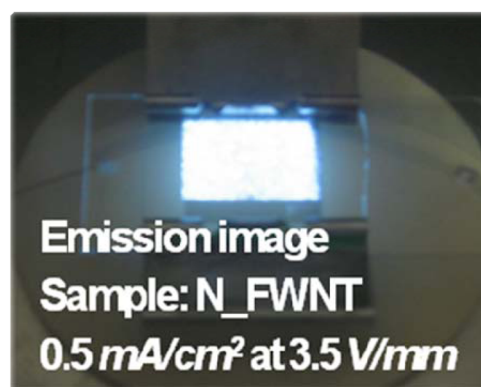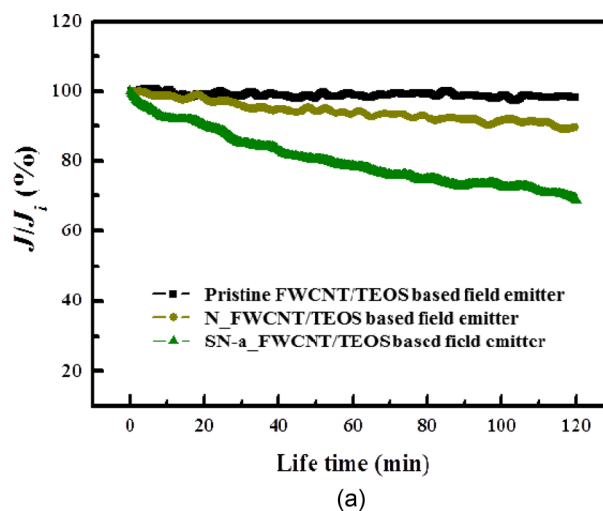
Fig. 10. (a) Emission current stability of the pristine FWCNT/TEOS and oxidized FWCNTs/TEOS based field emitters for 2 h at constant voltage. (b) Digital photo-image of emission pattern for N_FWCNT/TEOS based field emitter with a size of 2 cm × 2 cm (the corresponding emission current was 0.5 mA/cm²). FWCNT: few-walled carbon nanotube, TEOS: tetraethyl orthosilicate.

several papers to explain this phenomenon [30,31]. In our case, we can claim that this is related to desorption at a high electric field. At a high electric field, the emission current increases, and thus Joule heating occurs especially at the nanotube tip. In general, intrinsic nanotube emission properties are revealed after desorption of water molecules. However, water absorption is favorable to acid-treated nanotubes due to the polar-polar interaction between functional groups and water molecules. That is why pristine FWCNTs do not have a hetero-behavior of the field emission.

We have also compared the emission current stability of oxidized FWCNT-based field emitters with that of pristine FWCNT-based field emitters with a constant field at 0.35 mA/cm² of current density for 2 h. Fig. 10a shows the degradation rate of the emission current density (*J/J*ᵢ) at the constant field as a function of time. We found that the emission stability is dramatically enhanced by using the TEOS binder for improving the adhesion of CNTs to the substrate. We also note that the current degradation rate of N_FWCNT-based field emitters is similar to

that of pristine FWCNT-based field emitters, even though the initial current density of pristine FWCNTs is higher than that of N_FWCNTs. Moreover, we consider the emission current stability (J/J_i = 68.9% after 2 h) of the SN-a FWCNT-based field emitter to be the worst among the three samples. It is well known that the emission current of nanotubes decreases when a nanotube tip with attached residual oxygen gases is degraded by Joule heating under a high electric field [32]. In fact, the outgassing from the cathode is one of the main reasons for vacuum deterioration, resulting in degradation of the emission current. Even though the FWCNTs/TEOS thin films were annealed and cured at 150°C for 90 min, the residual oxygen gases are more favorably absorbed at the tip of acid-treated FWCNTs. Therefore, the current degradation rate of CNTs would mainly depend on the defect level of CNT tips, and thus we can conclude that the decreased emission current stability is mainly attributed to existence of defects on the nanotube surface, which can act as resistance to electron emission, and electrical stress loaded on defects, resulting in failure of field emission. The digital photo-image of the emission pattern from N_FWCNT/TEOS-based field emitter with a size of 2 cm × 2 cm is shown in Fig. 10b. We observed uniform and extremely bright electron emission from N_FWCNT using phosphor-coated ITO glass as an anode. This plane-type field emission, not spot-type, is attributed to the uniform length, diameter, and density of N_FWCNT-based field emitter.

4. Conclusions

We have discussed the influence of FWCNTs treated with nitric acid/sulfuric acid on field emission characteristics. Carboxyl and hydroxyl groups were functionalized on the surface of the FWCNTs using nitric acid and sulfuric acid in different proportions. When the FWCNTs are functionalized with carboxyl and hydroxyl groups, the dispersion stability in DMF was significantly enhanced due to the combination of polar-polar affinity and electrostatic repulsion.

In addition, FWCNTs/TEOS thin film field emitters were fabricated by a spray method using FWCNTs/TEOS one component solution onto ITO glass. After thermal curing, they were found tightly adhered to ITO glass, and after the activation process by a taping method, CNTs were aligned preferentially in the vertical direction. The FWCNTs/TEOS-based field emitter with uniform surface, small thickness and strong adhesion to the substrate was successfully fabricated using a spray method. The pristine FWCNT/TEOS-based field emitters revealed a higher current density, lower turn-on field, and higher field enhancement factor than the oxidized FWCNTs-based field emitters. However, the unstable dispersion of pristine FWCNTs in TEOS/DMF solution made them poorly applicable to field emitter fabrication using the spray method. Although the field emitter of nitric acid-treated FWCNT showed slightly lower field emission characteristics, this can be improved by introducing metal nanoparticles or a resistive layer coating.

Thus, we can conclude that our spray method could be useful for fabricating field emitters, which offer several advantages compared to previously reported techniques such as CVD and screen printing. For example, as well as a uniform surface, a

convenient method to deposit CNTs for cathodes, and good reproducibility, it is cost-effective and amenable to mass production, and it could potentially lead to the use of CNTs as functional devices.

References

[1] Iijima S. Helical microtubules of graphitic carbon. Nature, **354**, 56 (1991). http://dx.doi.org/10.1038/354056a0.

[2] Chernozatonskii LA, Gulyaev YV, Kosakovskaja ZJ, Sinitsyn NI, Torgashov GV, Zakharchenko YF, Fedorov EA, Val'chuk VP. Electron field emission from nanofilament carbon films. Chem Phys Lett, **233**, 63 (1995). http://dx.doi.org/10.1016/0009-2614(94)01418-U.

[3] Wang QH, Setlur AA, Lauerhaas JM, Dai JY, Seelig EW, Chang RPH. A nanotube-based field-emission flat panel display. Appl Phys Lett, **72**, 2912 (1998). http://dx.doi.org/10.1063/1.121493.

[4] Sohn JI, Lee S, Song YH, Choi SY, Cho KI, Nam KS. Patterned selective growth of carbon nanotubes and large field emission from vertically well-aligned carbon nanotube field emitter arrays. Appl Phys Lett, **78**, 901 (2001). http://dx.doi.org/10.1063/1.1335846.

[5] Sugie H, Tanemura M, Filip V, Iwata K, Takahashi K, Okuyama F. Carbon nanotubes as electron source in an x-ray tube. Appl Phys Lett, **78**, 2578 (2001). http://dx.doi.org/10.1063/1.1367278.

[6] Yue GZ, Qiu Q, Gao B, Cheng Y, Zhang J, Shimoda H, Chang S, Lu JP, Zhou O. Generation of continuous and pulsed diagnostic imaging x-ray radiation using a carbon-nanotube-based field-emission cathode. Appl Phys Lett, **81**, 355 (2002). http://dx.doi.org/10.1063/1.1492305.

[7] Bonard JM, Salvetat JP, Stockli T, Forró L, Chatelain A. Field emission from carbon nanotubes: perspectives for applications and clues to the emission mechanism. Appl Phys A: Mater Sci Process, **69**, 245 (1999). http://dx.doi.org/10.1007/s003390050998.

[8] De Jonge N. Brightness of carbon nanotube electron sources. J Appl Phys, **95**, 673 (2004). http://dx.doi.org/10.1063/1.1632551.

[9] Utsumi T. Vacuum microelectronics: what's new and exciting. IEEE Trans Electron Devices, **38**, 2276 (1991). http://dx.doi.org/10.1109/16.88510.

[10] Wei Y, Xie C, Dean KA, Coll BF. Stability of carbon nanotubes under electric field studied by scanning electron microscopy. Appl Phys Lett, **79**, 4527 (2001). http://dx.doi.org/10.1063/1.1429300.

[11] Purcell ST, Vincent P, Journet C, Binh VT. Hot nanotubes: stable heating of individual multiwall carbon nanotubes to 2000 K induced by the field-emission current. Phys Rev Lett, **88**, 105502 (2002). http://dx.doi.org/10.1103/PhysRevLett.88.105502.

[12] Choi WB, Chung DS, Kang JH, Kim HY, Jin YW, Han IT, Lee YH, Jung JE, Lee NS, Park GS, Kim JM. Fully sealed, high-brightness carbon-nanotube field-emission display. Appl Phys Lett, **75**, 3129 (1999). http://dx.doi.org/10.1063/1.125253.

[13] Uemura S, Yotani J, Nagasako T, Kurachi H, Yamada H, Ezaki T, Maesoba T, Nakao T, Saito Y, Yumura M. 39.4: large size FED with carbon nanotube emitter. SID Symposium Digest of Technical

Papers, **33**, 1132 (2002). http://dx.doi.org/10.1889/1.1830144.

[14] Saito Y, Nakahira T, Uemura S. Growth conditions of double-walled carbon nanotubes in arc discharge. J Phys Chem B, **107**, 931 (2003). http://dx.doi.org/10.1021/jp021367o.

[15] Jeong HJ, Kim KK, Jeong SY, Park MH, Yang CW, Lee YH. High-yield catalytic synthesis of thin multiwalled carbon nanotubes. J Phys Chem B, **108**, 17695 (2004). http://dx.doi.org/10.1021/jp046152o.

[16] Jeong HJ, Choi HK, Kim GY, Song YI, Tong Y, Lim SC, Lee YH. Fabrication of efficient field emitters with thin multiwalled carbon nanotubes using spray method. Carbon, **44**, 2689 (2006). http://dx.doi.org/10.1016/j.carbon.2006.04.009.

[17] Ham HT, Choi YS, Chung IJ. An explanation of dispersion states of single-walled carbon nanotubes in solvents and aqueous surfactant solutions using solubility parameters. J Colloid Interface Sci, **286**, 216 (2005). http://dx.doi.org/10.1016/j.jcis.2005.01.002.

[18] Hesse R, Streubel P, Szargan R. Improved accuracy of quantitative XPS analysis using predetermined spectrometer transmission functions with UNIFIT 2004. Surf Interface Anal, **37**, 589 (2005). http://dx.doi.org/10.1002/sia.2056.

[19] Chen L, Pang XJ, Qu MZ, Zhang Qt, Wang B, Zhang BL, Yu ZL. Fabrication and characterization of polycarbonate/carbon nanotubes composites. Composites Part A: Appl Sci Manuf, **37**, 1485 (2006). http://dx.doi.org/10.1016/j.compositesa.2005.08.009.

[20] Kim UJ, Furtado CA, Liu X, Chen G, Eklund PC. Raman and IR spectroscopy of chemically processed single-walled carbon nanotubes. J Am Chem Soc, **127**, 15437 (2005). http://dx.doi.org/10.1021/ja052951o.

[21] Sandler J, Shaffer MSP, Windle AH, Halsall MP, Montes-Moran MA, Cooper CA, Young RJ. Variations in the Raman peak shift as a function of hydrostatic pressure for various carbon nanostructures: a simple geometric effect. Phys Rev B, **67**, 35417 (2003). http://dx.doi.org/10.1103/PhysRevB.67.035417.

[22] Yu J, Grossiord N, Koning CE, Loos J. Controlling the dispersion of multi-wall carbon nanotubes in aqueous surfactant solu-tion. Carbon, **45**, 618 (2007). http://dx.doi.org/10.1016/j.carbon.2006.10.010.

[23] Huang W, Taylor S, Fu K, Lin Y, Zhang D, Hanks TW, Rao AM, Sun YP. Attaching proteins to carbon nanotubes via diimide-activated amidation. Nano Lett, **2**, 311 (2002). http://dx.doi.org/10.1021/nl010095i.

[24] Ausman KD, Piner R, Lourie O, Ruoff RS, Korobov M. Organic solvent dispersions of single-walled carbon nanotubes: toward solutions of pristine nanotubes. J Phys Chem B, **104**, 8911 (2000). http://dx.doi.org/10.1021/jp002555m.

[25] Graybeal JD. Molecular Spectroscopy, McGraw-Hill, New York (1988).

[26] Solymar L, Walsh D. Electrical Properties of Materials. 6th ed., Oxford University Press, Oxford (1998).

[27] Fursey G. Field Emission in Vacuum Microelectronics, Kluwer Academic/Plenum Publishers, New York (2005).

[28] Fursey GN, Glazanov DV. Deviations from the Fowler-Nordheim theory and peculiarities of field electron emission from small-scale objects. J Vac Sci Technol B, **16**, 910 (1998). http://dx.doi.org/10.1116/1.589929.

[29] Bonard JM, Salvetat JP, Stockli T, De Heer WA, Forro L, Chatelain A. Field emission from single-wall carbon nanotube films. Appl Phys Lett, **73**, 918 (1998). http://dx.doi.org/10.1063/1.122037.

[30] Rajalakshmi N, Dhathathreyan KS, Govindaraj A, Satishkumar BC. Electrochemical investigation of single-walled carbon nanotubes for hydrogen storage. Electrochim Acta, **45**, 4511 (2000). http://dx.doi.org/10.1016/s0013-4686(00)00510-7.

[31] Kung SC, Hwang KC, Lin IN. Oxygen and ozone oxidation-enhanced field emission of carbon nanotubes. Appl Phys Lett, **80**, 4819 (2002). http://dx.doi.org/10.1063/1.1485315.

[32] im SC, Choi YC, Jeong HJ, Shin YM, An KH, Bae DJ, Lee YH, Lee NS, Kim JM. Effect of gas exposure on field emission properties of carbon nanotubes arrays. Adv Mater, **13**, 1563 (2001). http://dx.doi.org/10.1002/1521-4095(200110)13:20<1563::aid-adma1563>3.0.co;2-h.